

# Whi3, a Developmental Regulator of Budding Yeast, Binds a Large Set of mRNAs Functionally Related to the Endoplasmic Reticulum\*<sup>§</sup>◆

Received for publication, June 17, 2008, and in revised form, July 28, 2008. Published, JBC Papers in Press, July 29, 2008, DOI 10.1074/jbc.M804604200

Neus Colomina<sup>1,2</sup>, Francisco Ferrezuelo<sup>1,2</sup>, Hongyin Wang<sup>3</sup>, Martí Aldea, and Eloi Garí<sup>4</sup>

From the Departament de Ciències Mèdiques Bàsiques, Institut de Recerca Biomèdica de Lleida, Universitat de Lleida, Montserrat Roig 2, 25008 Lleida, Catalonia, Spain

Whi3 is an RNA-binding protein associated with the endoplasmic reticulum (ER) that binds the *CLN3* mRNA and plays a key role in the efficient retention of cyclin Cln3 at the ER. In the present work, we have identified new Whi3-associated mRNAs by a genomic approach. A large and significant number of these Whi3 targets encode for membrane and exocytic proteins involved in processes such as transport and cell wall biogenesis. Consistent with the genomic data, we have observed that cell wall integrity is compromised in Whi3-deficient cells and found strong genetic interactions between *WHI3* and the cell integrity pathway. Whi3-associated mRNAs are enriched in clusters of the tetranucleotide GCAU, and mutation of the GCAU clusters in the *CLN3* mRNA caused a reduction in its association to Whi3, suggesting that these sequences may act as *cis*-determinants for binding. Our data suggest that Whi3 is involved in the regulation and/or localization of a large subset of mRNAs functionally related to the ER and, since it is important for different molecular processes such as cytoplasmic retention or exocytic traffic of proteins, we propose that Whi3 is a general modulator of protein fate in budding yeast.

RNA-binding proteins are involved in posttranslational regulation affecting diverse aspects such as stability, translation, and transport of mRNAs (1). Different data from genomic array analysis revealed that RNA-binding proteins associate with discrete subpopulations of the total mRNAs in the cell (2, 3). Particular mRNA-binding proteins would regulate mRNAs from different subpopulations of functionally related genes (4), which have been referred to as posttranscriptional operons (5).

\* This work was funded by grants from the Ministry of Education and Science of Spain (Consolider-Ingenio 2010), the Fundació La Caixa, and the European Union (Fondos FEDER). The costs of publication of this article were defrayed in part by the payment of page charges. This article must therefore be hereby marked "advertisement" in accordance with 18 U.S.C. Section 1734 solely to indicate this fact.

◆ This article was selected as a Paper of the Week.

The microarray data have been deposited in the ArrayExpress data base with accession number E-MEXP-1734.

§ The on-line version of this article (available at <http://www.jbc.org>) contains a supplemental table with nine worksheets.

<sup>1</sup> These authors contributed equally to this work.

<sup>2</sup> N. C. and F. F. are researchers of the Ramón y Cajal program.

<sup>3</sup> Present address, Department of Molecular Genetics and Microbiology, The State University of New York (SUNY), Stony Brook, NY 11794-5222.

<sup>4</sup> To whom correspondence should be addressed: Dept. Ciències Mèdiques Bàsiques, Facultat de Medicina, Universitat de Lleida, Montserrat Roig 2, 25008 Lleida, Catalunya, Spain, Tel.: 34-973702411; Fax: 34-973702426. E-mail: [eloi.gari@cmb.udl.cat](mailto:eloi.gari@cmb.udl.cat).

The transport and local translation of mRNAs are key steps in the regulation of protein localization (6, 7). The majority of mRNAs encoding secreted and membrane-bound proteins are translated in polysomes associated with the ER<sup>5</sup> membrane (8). Some of these proteins show a signal peptide sequence in the N terminus that is rapidly recognized by the signal recognition particle (SRP) after translation initiation. The SRP binds to a receptor localized in the ER membrane facilitating the association of the polysomes to the ER and facilitating the internalization of the nascent protein across the ER membrane by a translation-coupled mechanism. However, by using subcellular fractionation and genomic analysis, a large number of ER-associated mRNAs have been identified that encode proteins without a signal peptide tag (9). Since SRP-deficient cells are viable and still have sufficient levels of protein synthesis on the ER (10), specific determinants in the mRNA-containing ribonucleoproteins have been hypothesized that would recognize protein receptors at the ER surface (11). As an example of an SRP-independent mechanism, the RNA-binding proteins She2/3 recruit a significant set of mRNAs to the ER as a key step for efficient transport of the associated mRNAs to the bud (12–14).

Whi3 is an ER-associated protein that contains a C-terminal RNA recognition motif (RRM), being functionally involved in cell size and cell cycle regulation (15). Whi3 binds to the mRNA of *CLN3* (16), the most upstream activator of cell cycle entry in *Saccharomyces cerevisiae* (17, 18), with no obvious effects on mRNA or protein levels. Cln3 is mostly ER-associated in early G<sub>1</sub> cells and accumulates in the nucleus in late G<sub>1</sub> (19, 20). Whi3 is important for efficient retention of Cln3 at the ER in early G<sub>1</sub> and prevents unscheduled nuclear accumulation of Cln3. On the other hand, Whi3 interacts with the Cdc28 kinase, and we have proposed that Whi3 confines translation of Cln3 in the ER to efficiently retain newly formed Cln3-Cdc28 complexes (19). Whi4, which displays some similarities in the RRM and Cter regions (15), seems to play a partially redundant role to Whi3 in cell size control (15, 21). In addition to cell size regulation, Whi3 is essential for filamentous growth, but the effectors and targets of Whi3 in this process are unknown (22). The

<sup>5</sup> The abbreviations used are: ER, endoplasmic reticulum; CDK, cyclin-dependent kinase; RRM, RNA recognition motif; SRP, signal recognition particle; 3-HA, three-hemagglutinin; IP, immunoprecipitation; SGD, *Saccharomyces Genome Data base*; TAP, tandem affinity purification.

role of Whi3 in cell filamentation is dependent on the presence of the RRM motif and is largely independent of Cln3 function (16, 19), suggesting the existence of additional Whi3 targets.

Polysome partitioning between cytosol and ER serves to direct proteins to different compartments in eukaryotic cells, and the existence of different pathways for RNA traffic to the ER is widely accepted (8, 11). Whi3 is an RNA-binding protein associated to the ER, which makes it an interesting candidate for mRNA partitioning. In this work, we have used a genomic approach to identify new mRNA targets of Whi3, and we have obtained a list of more than 300 candidates that includes the mRNA of *CLN3*. The analysis of the data revealed that a significant number of Whi3-associated mRNAs encode for membrane and exocytic proteins, suggesting that Whi3 is involved in the regulation of ER-associated mRNAs. Since Whi3 is involved in ER-mediated retention and traffic of proteins, we hypothesize that Whi3 would localize mRNA translation at the ER and act as a general modulator of protein fate in budding yeast.

## EXPERIMENTAL PROCEDURES

**Yeast Strains, Plasmids, and Growth Conditions**—Strains used in pull-down experiments are SC0000 (*MATa ade2 arg4 leu2-3,112 ura3-52 trp1-289*) derivatives and were obtained from Euroscarf. Strains used in functional analysis derive from our parental strain CML128 (*MATa leu2-3,112 ura3-52 trp1-1 his4 canI-r*) (23). Yeast cell cultures and genetic manipulations were carried out as described (24–26), and DNA manipulations were performed by standard methods (27). Yeast cells were routinely grown in rich medium (YPD; 1% yeast extract, 2% peptone, and 2% dextrose) at 30 °C unless stated otherwise. Where needed, sorbitol was added to a final concentration of 0.8 M. Calcofluor White (Sigma) was used at a final concentration of 8  $\mu$ g/ml. Congo Red (Sigma) was added to a final concentration of 10  $\mu$ g/ml. For selection of plasmid-borne markers, yeast cells were grown in minimal medium (SD; 0.67% yeast nitrogen base and 2% dextrose), and supplements were added as required. Plasmid YEP352-*SLT2-3HA* (H. Torres) harbors the corresponding open reading frame under its own promoter into a 2 $\mu$ -based multicopy vector. Plasmid pCM194 is a YCplac33 derivative that contains three-hemagglutinin (3HA)-tagged *CLN3* open reading frame under the control of its own promoter (23). The *CLN3*<sup>mGCAU</sup> allele was obtained by *in vitro* synthesis (Genecust-Biobasic) and cloned by *in vivo* recombination in pCM194. In previous work, we have demonstrated that the 3'-untranslated region, containing two GCAU tetranucleotides, is not relevant for the Whi3 regulation (16, 19). Details of strain and plasmid constructions are available upon request.

**Affinity Purification Procedure**—The method for extract preparation was adapted from Rigaut *et al.* (28) as described (16). Briefly, extracts were prepared from 1 liter of yeast cells grown to log phase ( $A_{600} = 1$ ). Cells harboring centromeric plasmids were grown initially in selective minimal medium, diluted in YPD medium, and grown more than 8 h. Cell growth was halted by adding ice into the culture, and all subsequent steps were performed at 4 °C. Buffer A (10 mM K-Hepes, pH 7.9,

10 mM KCl, 1.5 mM MgCl<sub>2</sub>, 0.5 mM dithiothreitol, and protein inhibitors) was added to frozen pellets, and cells were broken by passing them twice through a French press. The extract was adjusted to a final concentration of 200 mM KCl and 1% Triton and then centrifuged at 4500  $\times$  *g* for 2 min. Samples for input RNA and protein were taken from the supernatant at this step. The remaining extract was added to a column containing 100  $\mu$ l of Sepharose-IgG beads (Amersham Biosciences), allowing the liquid to drain by gravity flow. Beads were quickly washed twice with IPP150 (10 mM Tris-Cl, pH 8, 150 mM NaCl, 0.1% Triton), allowing the buffer to drain by gravity flow. Finally, washed IgG beads were eluted directly with 1 ml of TRIzol (Invitrogen). Input and IP RNAs were purified by using the PureLink total RNA purification system kit (Invitrogen).

**Microarrays Analysis**—cDNA was synthesized from 10–15  $\mu$ g of input RNA or 0.7–1  $\mu$ g of IP RNA. An indirect labeling method with amino-allyl-dUTP (Ambion) was used as described previously with slight modifications (29). We used priming from both an anchored oligo(dT)<sub>20</sub> primer and random hexamers (Invitrogen). As we had multiple independent IPs for each strain, we labeled some IPs with Cy5 and their corresponding inputs with Cy3 and *vice versa*. The Cy3- and Cy5-labeled cDNAs (IP *versus* input) were mixed and hybridized to spotted DNA microarrays, which will be described in detail elsewhere.<sup>6</sup> Briefly, our arrays contained PCR-amplified DNA fragments targeting  $\sim$ 5800 *S. cerevisiae* genes (including 56 small nucleolar RNAs and small nuclear RNAs). Also, arrays contained probes targeting the 3'-untranslated region of some 500 genes in addition to the open reading frame-targeting probe. Most cell cycle-regulated genes described by Spellman *et al.* (30) were spotted four times at different locations in the array to assess for spot consistency. Microarrays were scanned with an Axon GenePix 4100A scanner (MDS Analytical Technologies), and data were generated with the GenePix Pro 5 software. We performed a visual quality control to flag abnormally looking spots. Then, spots with low signal-to-noise ratios (<3) in both channels, and those with fewer than 60 pixels were removed. Arrays were normalized by an intensity-dependent method (print-tip loess) implemented in the GEPAS package on the web (31). Median pixel intensities and background subtraction were used, and the software produced normalized log<sub>2</sub> ratios (IP/input) of the median pixel intensity for each spot. For duplicated spots in the array, inconsistent spots as defined by having a value departing more than 0.5 from their median were removed, and the median of consistent duplicated spots was taken as representative value for that gene. We selected as candidate targets those genes that were in the 90 percentile or higher in at least four of the six Whi3-IPs. This amounted to 340 probes targeting 337 genes. Of these, we removed 11 genes that passed this selection criterion in the mock IPs.

**Miscellaneous**—We have used a signal amplification method to detect endogenous levels of Cln3-3HA by immunofluorescence (16). Slides were sequentially incubated with rat anti-HA

<sup>6</sup> F. Ferrezuelo, M. Aldea, and B. Futcher, manuscript in preparation.

## mRNA Targets of the Cell Development Regulator Whi3

(clone 3F10, Roche Applied Science) and goat anti-rat and rabbit anti-goat antibodies labeled with Alexa Fluor 555 (Molecular Probes). To analyze nuclear accumulation of Cln3, Image J software was used to set a threshold to outline the cytoplasm of most cells in the immunofluorescence image. The threshold was increased 2-fold, and outlined regions were scored as positive nuclei by visual comparison with a stacked 4',6-diamidino-2-phenylindole image.

Yeast cells growing exponentially in YPD at  $A_{600} < 0.5$  were used to obtain cell volume distributions with a Z2 Coulter counter (16). Cells harboring centromeric plasmids were grown initially in selective minimal medium, diluted in YPD medium, and grown overnight.

Protein extracts and Western blot analysis with mouse anti-HA (clone 12CA5) and anti-phospho-P44/P42 (New England Biolabs) antibodies were performed as described previously (23, 32). TAP-tagged proteins were detected with a peroxidase-labeled rabbit anti-peroxidase antibody-soluble complex (Sigma) (28). Protein concentration in supernatants was determined by a Micro DC protein assay (Bio-Rad), and equivalent amounts of total protein extracts were run on SDS-polyacrylamide gels. Chemiluminescent detection was performed using a Lumi-Imager system (Roche Applied Science).

### RESULTS

**Identification of mRNAs Associated with Whi3**—To identify mRNAs associated with Whi3, we performed pull-down experiments with a Whi3-TAP-tagged strain (16). This procedure yielded sufficient RNA for labeling without amplification by reverse transcription-PCR (3, 33). Whi3-associated mRNAs and total RNA were used to produce labeled cDNAs and then mixed and hybridized to DNA microarrays. The same procedure was performed with untagged cells as control (mock). We performed six independent experiments with the Whi3-TAP strain and five with the untagged strain (supplemental Table S1). As expected for a specific capture in pull-down experiments, the distribution of mRNAs bound to Whi3 showed an asymmetric pattern (Fig. 1). Approximately 3.7% of mRNAs were situated beyond two positive standard deviations compared with only a 0.95% of mRNAs beyond two negative standard deviations. On the contrary, the distribution of the mock isolates was symmetrical, indicating irrelevant enrichment of mRNAs. In a previous work, we had described the specific interaction of the *CLN3* mRNA with the Whi3 protein (16). In the arrays, which contained four *CLN3* spots distributed at different locations, the mRNA of *CLN3* was clearly enriched in all the Whi3-TAP samples with an average  $\log_2$  ratio of 1.98, whereas in the mock samples, the average  $\log_2$  ratio was  $-0.03$  (Fig. 1). Moreover, this enrichment was repetitive and consistent in all the *CLN3* spots among the different experiments, giving strong support to the validity of our results. To define a group of targets specific to Whi3, we applied a ranking approach by selecting those genes that were in the 90 percentile or higher in at least four of the six Whi3-IPs. Following the same criterion, we only found 11 sequences of small nucleolar RNAs that were also consistently enriched in the mock sample. After removal of these mock sequences, we

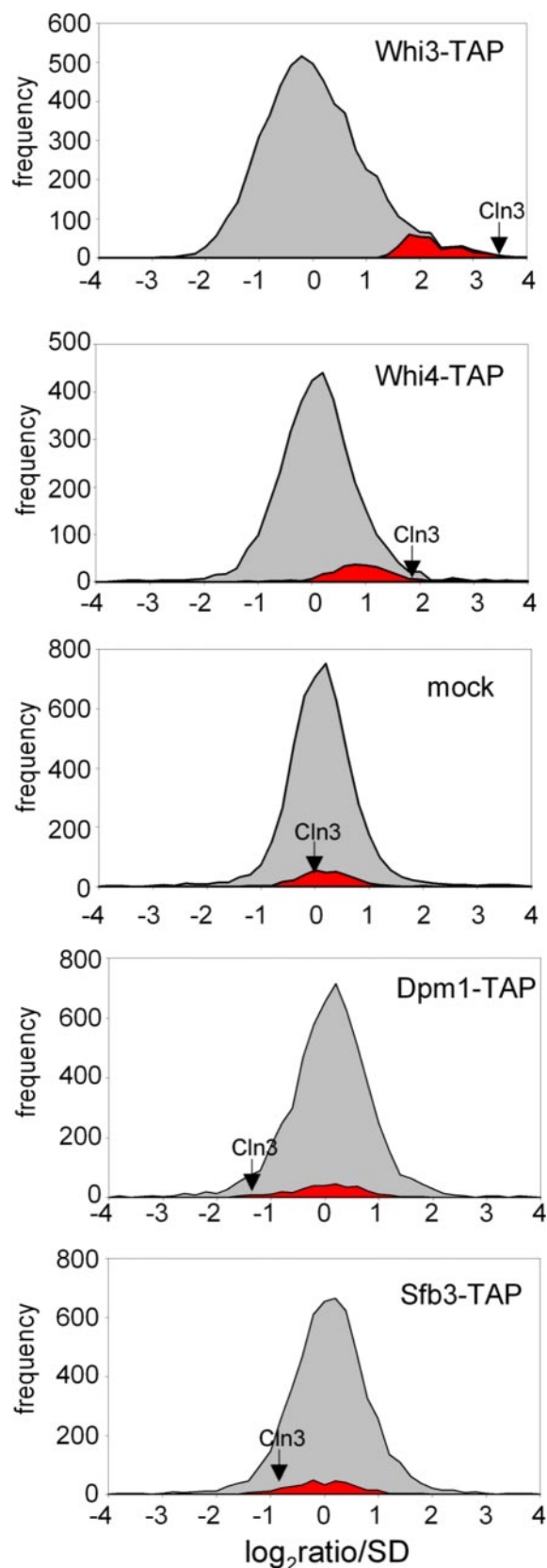


**FIGURE 1. Pull-down distributions.** Distributions of  $\log_2$  ratios obtained by averaging all independent microarray hybridization experiments for each strain, wild type (SC0000), and the TAP-tagged versions of Whi3 (SC3304), Whi4 (SC3411), Dpm1 (SC1622), and Sfb3 (SC2482) are shown. Values are plotted scaled to the population standard deviations. The distribution of selected Whi3 targets is shown in red, and the position of *CLN3* is marked by an arrow.

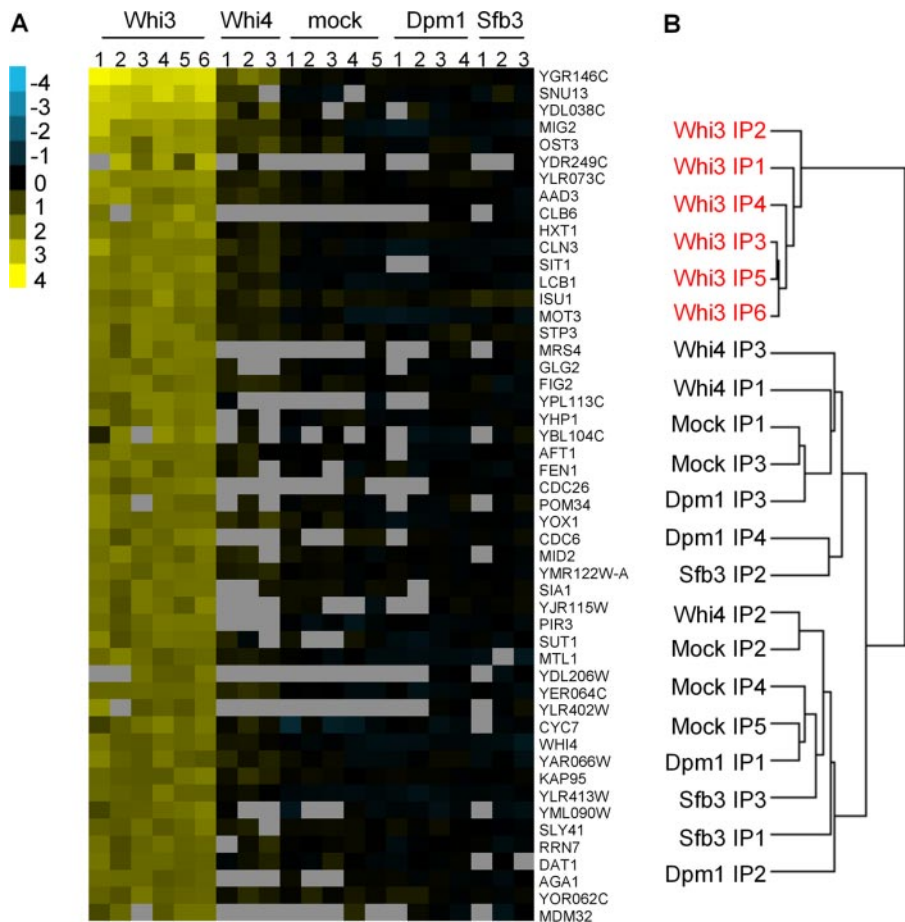


**FIGURE 2. Identification of *Whi3*-associated mRNAs.** *A*, TreeView generated heat map showing the top 50 candidate targets for *Whi3*. Genes are in rows; independent replicate IPs are in columns. Yellow denotes enrichment in the IP relative to the input RNA. Log<sub>2</sub> ratio values are plotted. *B*, correlation analysis of all the arrays performed in this study. The software Cluster 3.0 (51) was used to cluster arrays using an uncentered Pearson correlation similarity metric and average linkage. Other metrics gave similar results. Java TreeView was used to generate the tree.

obtained a list with 326 enriched mRNAs in our *Whi3*-TAP samples (Fig. 2*A*; supplemental Table S1). Consistently, *CLN3* was located among the top 20 candidates. The consistency of the list was highly reproducible independently of the application of other statistical methods for selection and cutoff.<sup>7</sup>

We also applied the same pull-down analysis to determine the target mRNAs for *Whi4*, which shares some structural and functional similarities with *Whi3* (15). In three independent experiments using the *Whi4*-TAP strain, we obtained lower signals in the microarray, perhaps due to the lower amounts of *Whi4* in the pull-down samples when compared with *Whi3* (data not shown). Nonetheless, the genes enriched in *Whi3* experiments were also slightly enriched in *Whi4* pull-down samples (Figs. 1 and 2*A*). In agreement with this result, *Whi3* and *Whi4* show partial functional redundancy as deduced from their phenotypical analysis (Refs. 15 and 21 and see below).

Many mRNAs selected by their association to *Whi3* encode membrane- and ER-associated proteins (see below). Given that *Whi3* is localized in ER fractions (20), the enrichment in the

pull-down sample could be caused by the presence of contaminant ER structures bound to *Whi3*. To exclude this possibility, we used two strains harboring the ER-associated proteins *Dpm1* and *Sfb3* tagged with the TAP epitope as controls. We carried out four pull downs with the *Dpm1*-TAP strain and three pull downs with the *Sfb3*-TAP strain (supplemental Table S1). The protein *Dpm1* contains a transmembrane domain that is anchored to the ER. *Dpm1* was insoluble in our non-denaturing extracts and undetectable in the supernatant of cell extracts after centrifugation (see “Experimental Procedures”) (data not shown), indicating the absence of contaminating ER membranes in the extracts. Microarray analysis of *Dpm1*-TAP pull-downs produced very similar results to those obtained with the untagged strain and, accordingly, *Whi3* targets were not found significantly enriched (Figs. 1 and 2*A*). *Sfb3* was soluble in non-denaturing extracts, perhaps due to the fact that it associates to the cytoplasmic face of the ER and was detected in the pull-down samples (data not shown). Despite that, the distribution of mRNAs in the pull downs with this strain was also similar to the untagged strain as shown by cluster analysis (Fig. 2*B*),

being that the *Whi3* targets are not enriched either (Figs. 1 and 2*A*). Additionally, we compared our list of genes with available data for mRNAs bound to She proteins (14). These proteins are associated to the ER and are required to transport several mRNAs to the bud. The majority of *Whi3* targets were not found among those bound by She proteins (data not shown), which further supports the specificity of our pull-down analysis with the *Whi3*-TAP strain.

*Whi3* Significantly Binds mRNAs Encoding Membrane and Exocytic Proteins—To gain insight into the function of *Whi3* as an RNA-binding protein, we classified the *Whi3*-associated transcripts by the subcellular localization of their coded products according to the MIPS yeast genome data base (34) and the *Saccharomyces* Genome Data base (SGD) (35). Out of the 326 *Whi3*-associated transcripts, the localization data were available for 306 candidates, which were categorized in five distinct cell compartments similarly as described previously by Kumar *et al.* (36) (Fig. 3*A*). Remarkably, the exocytosis network and plasma membrane compartments were substantially enriched in comparison with the entire yeast genome. The exocytosis network is a broad compartment that includes proteins localized in the ER and along the secretory pathway but also a large

<sup>7</sup> N. Colomina, F. Ferrezuelo, H. Wang, M. Aldea, and E. Garí, unpublished data.

## mRNA Targets of the Cell Development Regulator *Whi3*

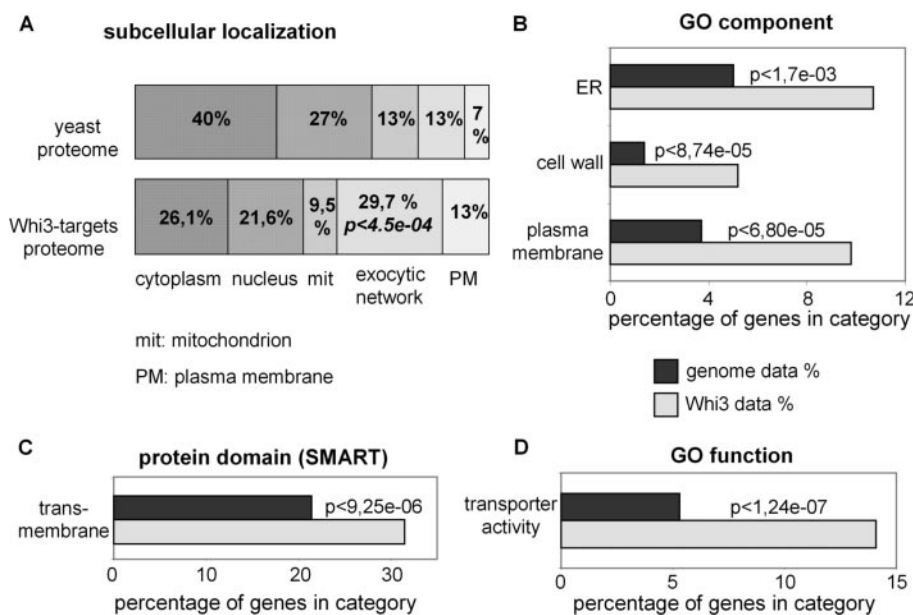


**FIGURE 3. Characterization of *Whi3* targets.** *A*, classification of proteins encoded for by the *Whi3*-associated mRNAs based on subcellular localization information gathered from MIPS (34) and SGD (35) data bases. The percentage of each compartment is indicated inside the chart. The percentages of the yeast proteome were obtained from Kumar *et al.* (36). The significance in the enrichment ( $p$  value) of the exocytosis network was obtained from the FunSpec data base (52). *B*, genes in the *Whi3* data set were classified by cellular component terms (*GO component*) gathered from SGD data base (see supplemental Table S1). *C*, analysis of the predicted transmembrane domains in the *Whi3* data set by the Simple Modular Architecture Research Tool (SMART) domain data base (52, 53) (see supplemental Table S1, *funSpec data*). *D*, *Whi3* targets encode for proteins involved in transport. Genes in the *Whi3* data set were classified by biological function terms (*GO function*) gathered from the SGD data base (see supplemental Table S1). *B*, *C*, and *D*, the comparative enrichment in the various categories between the *Whi3* data set (gray columns) and the entire yeast genome (black columns) is depicted together with the significance values ( $p$  values).

number of secreted proteins finally localized in the cell periphery. In accordance with this, the analysis of the data in the Gene Ontology (GO) data base showed that the *Whi3* targets were significantly enriched in transcripts encoding proteins localized in the ER, cell wall, and plasma membrane (Fig. 3*B*). Concomitantly, our data showed that a relevant part of the proteins encoded by *Whi3*-associated transcripts contain a transmembrane domain (Fig. 3*C*), among them the 84.6% of plasma membrane targets and the 56% of exocytic network targets. A 21.5% of the proteins encoded by *Whi3* targets show a putative signal peptide tag (34, 35). This percentage rises to 50% for the targets grouped in the exocytosis network, indicating that a significant fraction of *Whi3* targets encodes for proteins likely translocated to the ER lumen. Then, the overall analysis of the data suggests that *Whi3* significantly binds transcripts encoding membrane and exocytic proteins. Assuming that the majority of these transcripts are translated in ER-associated polysomes, we propose that *Whi3* binds specifically to ER-associated mRNAs. This is in agreement with our previous result showing the association of *Whi3* to the ER fraction (20).

We also used the Gene Ontology annotation for process and function to analyze the list of *Whi3* targets, which indicated that the encoded proteins participate in a broad spectrum of cell processes (supplemental Table S1). The most abundant group of *Whi3*-associated mRNAs encodes for proteins involved in transport (Fig. 3*D*). This group includes 52 mRNAs encoding classical membrane transporters and permeases and 18 transcripts involved in vesicle-mediated

transport. Additionally, other cell processes related to the cell periphery such as response to chemical stimulus (10.4%) and cell wall biogenesis (4.9%) are broadly represented among the *Whi3* targets. This is in accordance with the presence of an elevated number of membrane and exocytic proteins encoded by the *Whi3* targets.

A number of *Whi3* targets were also related to cell cycle progression. In particular, 27 (8.3%) mRNAs identified in *Whi3* pull downs encode for proteins involved in cell cycle regulation, being highly significant the presence of regulators of the cyclin-dependent kinases (CDKs) when compared with the whole genome ( $p < 2.47 \times 10^{-5}$ ) (supplemental Table S1). Besides *Cln3*, other cyclins such as *Cln2*, *Cln6*, and *Cln2* were also enriched in *Whi3* pull downs. On the other hand, 10 transcriptional factors such as *Yox1* or *Fkh2* that regulate different phases of the cell cycle were also identified. Furthermore, in agreement with the fact that *Whi3* uses N-terminal se-

quences to recruit *Cdc28* (19), 14 mRNAs enriched in *Whi3* pull downs encode for putative *Cdc28* substrates. Thus, *Whi3* associates to mRNAs that code for proteins functionally involved in diverse roles such as transport, signaling, and maintenance of cell integrity and cell cycle regulation.

***Whi3* Is Required for Maintenance of Cell Integrity**—Proficient exocytic traffic and membrane transport are required to maintain cell wall integrity (37). Among the *Whi3*-transcripts, we have identified 17 mRNAs encoding cell wall proteins involved in enzymatic and structural functions. Consequently, *Whi3* may be important to maintain cell integrity at least under some specific conditions of growth. Remarkably, the *Whi3* homologue in *Schizosaccharomyces pombe*, the RNA-binding protein *Scw1*, has been involved in the maintenance of cell wall structure (38, 39). To test whether *Whi3* is important in the control of cell integrity, we challenged *Whi3*-deficient cells with cell-wall inhibitory drugs such as Congo Red and Calcofluor White, which cause deleterious effects on growth (37). As shown in Fig. 4*A*, *whi3Δ* cells were more sensitive to Congo Red and Calcofluor White when compared with wild type. Moreover, this phenotype was dependent on the ability of *Whi3* to bind mRNAs since deletion of the RRM in *Whi3* produced the same growth defect. Although the *whi4Δ* mutant was as resistant as the wild type, the double *whi3Δwhi4Δ* mutant was much more sensitive to Congo Red and Calcofluor White when compared with the *whi3Δ* single mutant, reinforcing the idea that *Whi4* may play somewhat redundant roles with *Whi3*. Interestingly, both single *whi3Δ* and double *whi3Δwhi4Δ*

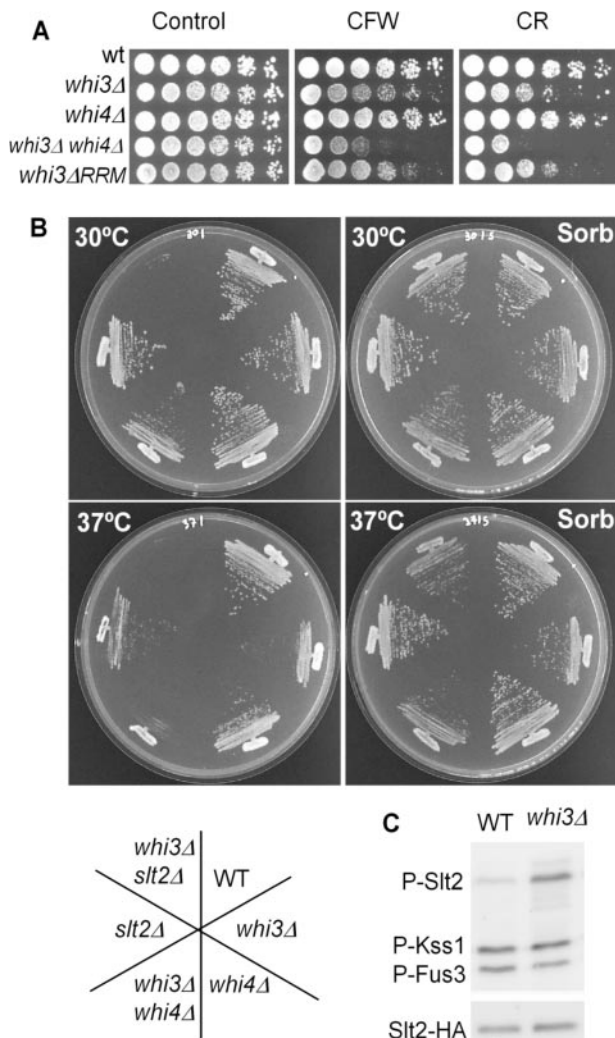


**FIGURE 4. *Whi3*-deficient cells show cell wall perturbations.** *A*, evaluation of growth sensitivity to Congo Red (CR) and Calcofluor White (CFW) drugs of wild-type (CML128), *whi3Δ* (CML217), *whi4Δ* (CML219), *whi3Δwhi4Δ* (CYC285), and *whi3ΔRRM* (CYC159) cells 3 days after plating a series of 5-fold diluted spots in rich medium. *B*, analysis of growth capacities at different temperatures and effects of 0.8 M sorbitol (Sorb) in wild-type (CML128), *whi3Δ* (CML217), *whi4Δ* (CML219), *whi3Δwhi4Δ* (CYC285), *slt2Δ* (CML399), and *whi3Δslt2Δ* (CYC287) cells streaked in rich medium. *C*, Western blot analysis of Slt2 phosphorylation in wild-type (CML128) and *whi3Δ* (CML217) cells harboring the Yep352-Slt2-3HA plasmid. Cell cultures were exponentially grown in minimal medium at 25 °C. Western blot analysis was performed to detect activated (*P-Slt2*) and total (*Slt2-3HA*) amounts of Slt2. *P-Kss1*, activated Kss1; *P-Fus3*, activated Fus3.

mutants exhibited a growth delay at 37 °C that was recovered by the addition of 0.8 M sorbitol (Fig. 4*B*), an unambiguous symptom of alterations in the protective cell cover. To confirm the existence of anomalies in the cell wall of *Whi3*-deficient cells, we evaluated phospho-Slt2 levels in the *whi3Δ* mutant. Phosphorylation of mitogen-activated protein (MAP) kinase Slt2 is induced through the cell integrity pathway in response to a broad spectrum of perturbations in the cell wall (32, 37). As expected, *whi3Δ* cells showed an increased level of phospho-Slt2 when compared with wild-type cells (Fig. 4*C*). To further evaluate the importance of *Whi3* in cell wall integrity, we combined the *whi3Δ* and *slt2Δ* mutations. This double mutant showed a synthetic lethal phenotype at 30 °C, which was rescued in the presence of 0.8 M sorbitol (Fig. 4*B*). The overall data

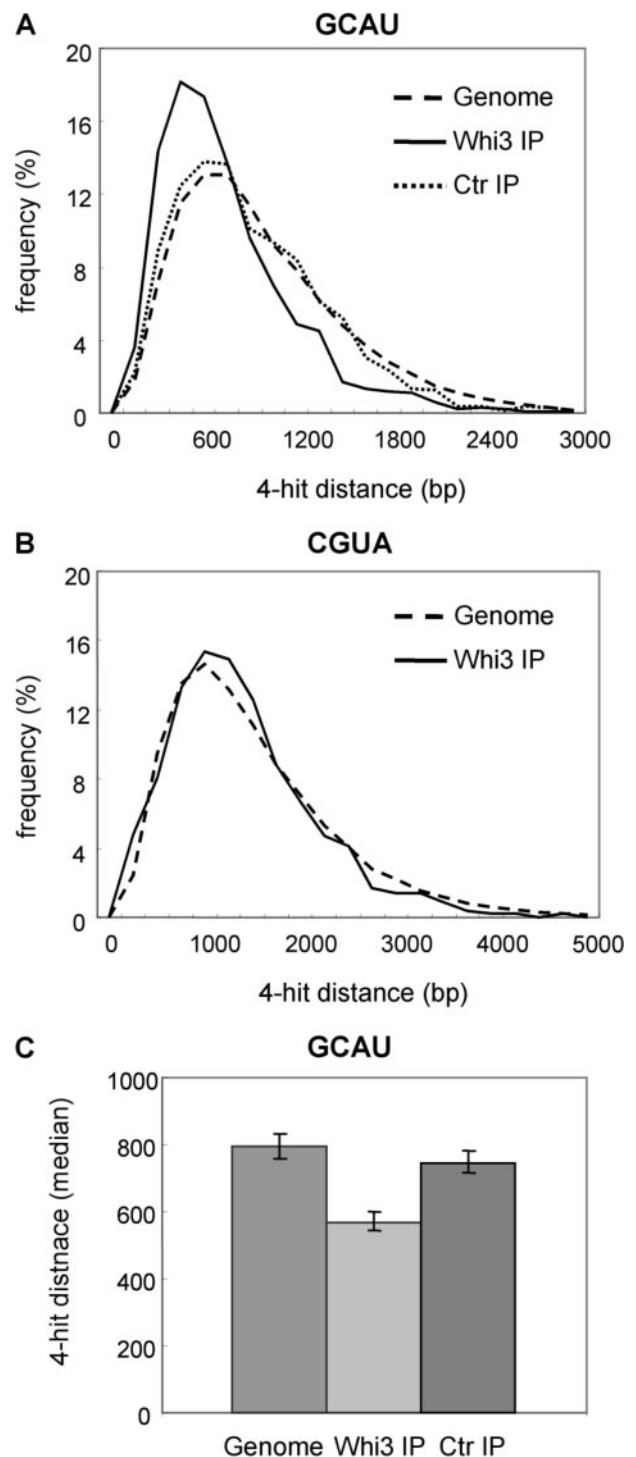


**FIGURE 5. *Whi3*-associated mRNAs are enriched in clusters of the GCAU tetranucleotide.** *A*, to quantify the enrichment in GCAU clusters, for each GCAU sequence in the mRNA, the distance to a third consecutive hit was measured. Graphs show the frequency of these distances in base pairs (which contain four consecutive GCAU hits) among the *Whi3* transcripts when compared with the same number of transcripts from mock pull down (Ctr IP) and the total genome. *B*, same as in *A* for the CGUA tetranucleotide sequence. *C*, the graph shows median and confidence limits for the median for each distribution plotted in *A*.

suggest that the absence of *Whi3* interferes with normal cell wall development and requires an active integrity pathway for survival.

## mRNA Targets of the Cell Development Regulator *Whi3*

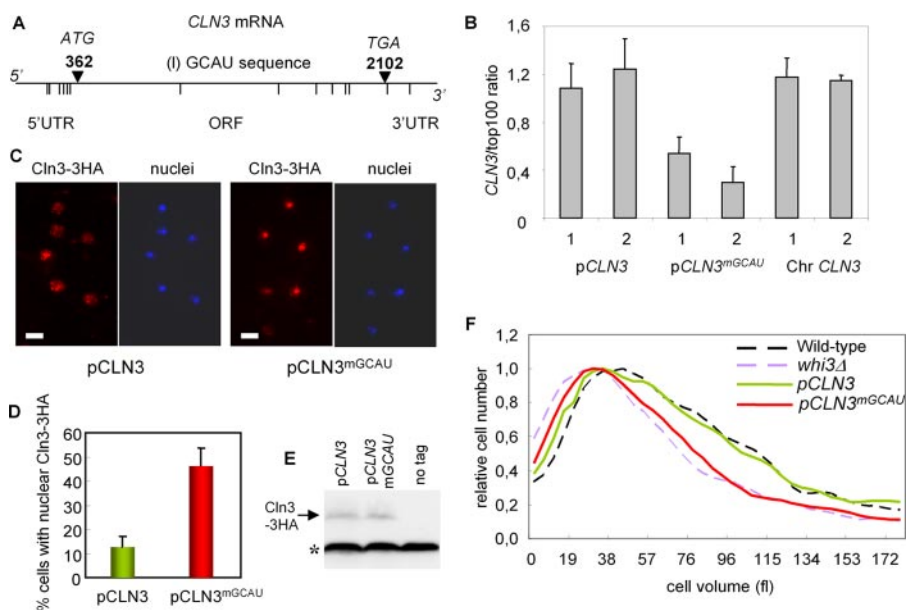


**FIGURE 6. Mutation of the GCAU clusters in the *CLN3* mRNA reduces the interaction with *Whi3*.** *A*, diagram representing the distribution of the 14 GCAU sequences (*dashes*) in the *CLN3* mRNA that were mutated to obtain the *CLN3*<sup>mGCAU</sup> allele. *UTR*, untranslated region; *ORF*, open reading frame. *B*, a *cln3Δ* *Whi3*-TAP (*CYC124*) strain transformed with plasmids expressing wild-type (*pCLN3*) and mutant (*pCLN3*<sup>mGCAU</sup>) mRNAs was used for microarray analysis of *Whi3*-TAP pull downs. *CLN3* ratios were made relative to the top hundred targets of *Whi3* obtained from experiments shown in Fig. 1. Two independent experiments for the wild-type chromosomal *CLN3* (*Chr CLN3*) are also shown. The values are obtained by averaging the four *CLN3* spots on each array. *Error bars* represent confidence limits of the mean. *C*, *cln3Δ* (*CML211*) cells expressing 3HA-tagged wild-type (*pCLN3*) and mutant (*pCLN3*<sup>mGCAU</sup>) constructs on centromeric vectors were grown exponentially and analyzed by immunofluorescence with an anti-HA antibody. Nuclei were detected by 4',6-diamidino-2-phenylindole staining. *Bar*, 5 μm. *D*, the percentage of cells (*n* = 300) with *Cln3*-3HA nuclear/cytoplasmic ratios higher than 2; confidence limits ( $\alpha$  = 0.01) are plotted. *E*, protein extracts of cells corresponding to *C* were analyzed by Western blot with an anti-HA antibody. The asterisk indicates an unspecific band. *F*, cell volume distributions of cells corresponding to *C*. Wild-type (*CML128*) and *whi3Δ* mutant (*CML217*) cells growing under the same conditions were used as internal controls.

*The GCAU Tetranucleotide Is a cis-Acting Determinant in the Whi3 Targets*—The consensus structure of the RRM is composed by a four-stranded antiparallel  $\beta$ -sheet domain that is able to directly interact with a maximum of four nucleotides in single-stranded nucleic acids (40). Remarkably, a three-hybrid screen using *Whi3* as RNA-binding bait yielded a large number of small RNA sequences with one or more copies of the GCAU tetranucleotide (41, 42).<sup>8</sup> Strikingly, the *CLN3* mRNA contains two regions with five GCAU sequences each, the first within a fragment of 150 nucleotides at the 5'-untranslated region and the second within 300 nucleotides at the 3' region of the open reading frame (19) (see Fig. 6A). We therefore carried out a comparative study of the presence and distribution of the GCAU sequences among the list of *Whi3*-associated transcripts, the mock isolates, and the whole genome. Our analysis revealed that the *Whi3*-associated mRNAs showed a significant enrichment in clusters formed by four GCAU sequences (Fig. 5, *A* and *C*). Although to a lesser extent, *Whi3* targets were also enriched in clusters with less than four GCAU tetranucleotides (data not shown). The same analysis using an unrelated tetranucleotide produced negative results, demonstrating the specificity of the GCAU enrichment (Fig. 5B). To establish the importance of these *in silico* data, we obtained by *in vitro* synthesis a *CLN3*<sup>mGCAU</sup> allele carrying mutations in the 14 GCAT

sites in the *CLN3* gene (Fig. 6A). Mutations within the open reading frame were conservative regarding codon meaning to preserve protein sequence. To analyze the efficiency of the *CLN3*<sup>mGCAU</sup> mRNA as *Whi3* target, we introduced 3HA-tagged *CLN3*<sup>mGCAU</sup> and wild-type alleles in a *cln3Δ* strain expressing a *Whi3*-TAP fusion and performed pull-down assays. To quantify relative binding efficiencies of mutant and wild-type mRNAs, *CLN3* log ratios were made relative to the average log ratio of the top 100 mRNAs in the *Whi3* target list. As shown in Fig. 6B, enrichment of the *CLN3*<sup>mGCAU</sup> mRNA in *Whi3* pull downs was greatly diminished when compared with the wild-type mRNA, demonstrating the importance of the GCAU sequences in the interaction with *Whi3*. *CLN3*<sup>mGCAU</sup> and wild-type mRNAs produced very similar levels of *Cln3* protein (Fig. 6E). However, most cells expressing the *CLN3*<sup>mGCAU</sup> mRNA showed a distinctive nuclear accumulation of *Cln3* when compared with cells carrying the wild-type mRNA (Fig. 6, *C* and *D*). More important, cells harboring the

*CLN3*<sup>mGCAU</sup> allele presented a reduction in cell volume similar to *Whi3*-deficient cells (Fig. 6F). Thus, the *CLN3*<sup>mGCAU</sup> allele recapitulates the main defects of the *whi3Δ* deletion regarding cell cycle control in G<sub>1</sub> and demonstrates the relevance of the GCAU tetranucleotide as a *cis*-acting determinant for *Whi3* binding.

## DISCUSSION

Here we have identified new mRNA targets associated to the RNA-binding protein *Whi3*. Analysis of *Whi3* targets revealed a significant enrichment of transcripts encoding membrane and exocytic proteins, being that many of these proteins are involved in cell processes such as transport and cell wall biogenesis. In accordance with this, we have observed that *Whi3*-deficient cells exhibit cell wall anomalies and found strong genetic interactions with elements of the cell integrity pathway. It is important to note that all cell wall proteins encoded for by *Whi3* targets show a signal peptide tag and therefore would be transported to the cell wall through the exocytic pathway. Previously, *Whi3* has also been involved in the exocytic pathway. The *whi3Δ* mutant shows a reduced fitness in combination with a deletion of *PEP3*, a gene encoding a subunit of class C vacuolar protein sorting complex (43). Class C vacuolar protein sorting complex regulates vesicle docking and fusion at the endosome and vacuole, and therefore, it is important in protein sorting.

<sup>8</sup> D. J. SenGupta, S. Fields, and M. Wickens, personal communication.

Overall, a strong correlation between the functional and structural characteristics of certain *Whi3* targets and the phenotypes of *Whi3*-deficient cells exists. *Whi3* could regulate stability and/or translation efficiency of their mRNA targets. However, by microarray analysis, we have observed that the levels of the vast majority of *Whi3*-associated mRNAs were unchanged in *Whi3*-deficient cells (data not shown). On the other hand, *Whi3* has no obvious effects on the levels of proteins encoded for by some mRNA targets (Ref. 16 and data not shown), suggesting that *Whi3* is not a universal regulator of mRNA stability or translation. Instead, we propose that *Whi3* would play a role in the regulation of their mRNA targets by localizing their translation at the cytosolic face of the ER and/or contributing to an efficient translocation across the ER of those encoded proteins destined to the exocytic pathway. Recent findings predict the existence of SRP-independent mechanisms to recruit mRNAs to the cytoplasmic surface of the ER and translocate the nascent protein into the ER lumen (8, 11). However, the presence of a significant number of *Whi3* targets harboring a signal peptide tag suggests the possibility that *Whi3* performs its function coordinated with SRP elements.

The stronger phenotype of the *whi3Δ* mutant is a complete inability to grow as filaments (22). Considering our present data, two different possibilities could explain this defect. On the one hand, filamentation needs active exocytic traffic and cell wall remodeling to maintain apical growth, both of which would require *Whi3* to direct mRNA targets to the ER as the start point of the exocytic pathway. On the other hand, we cannot exclude the involvement of *Whi3* in ER-coupled transport of mRNAs to the daughter cell as a key requirement for polarized growth. Similarly to *She* proteins, which transport to the bud mRNAs coding for essential elements involved in apical growth such as the GTPase *Cdc42* (12), *Whi3* binds some mRNAs coding for proteins that regulate apical growth and cell filamentation such as cyclin *Cln2* and transcription factor *Tec1*. Recruitment of these targets by *Whi3* could be important to drive them to the daughter cell and efficiently maintain cell filamentation. Intriguingly, among the *Whi3* targets, we also found the transcript coding for another RNA-binding protein, *Mpt5* (supplemental Table S1). This protein also binds the *TEC1* mRNA and modulates its translation (44). Conceivably, both *Mpt5* and *Whi3* could coordinately regulate *Tec1* function. Combinatorial action of different RNA-binding proteins has been proposed to be important to control mRNA translation and stability (5).

Among the *Whi3* targets, we have identified a considerable number of mRNAs encoding transcription factors that are not obviously related to ER functions. ER retention is important for regulation of transcription factor *Spt23* (45). This protein remains anchored at the cytoplasmic face of the ER, and it is released by a chaperone-dependent mechanism under inducing conditions. One of the identified *Whi3* target mRNAs codes for *Aft1*, a transcription factor that shows differential subcellular localization depending on iron availability (46). Heme is involved in proper *Aft1* activation. It is subject to turnover at the ER by *Hmx1*, allowing cells to use heme as a nutritional iron

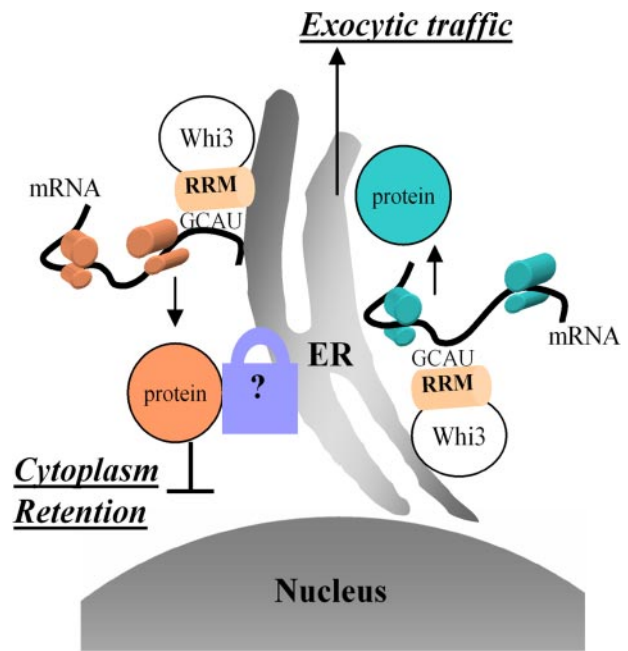


FIGURE 7. **Whi3 as a determinant of protein fate.** The diagram shows a speculative model summarizing data obtained. *Whi3* would bind ER-associated ribonucleoproteins containing specific mRNA targets enriched in GCAU clusters. For some of them, including *CLN3*, *Whi3* would be necessary for an efficient retention at the ER of the encoded products. Alternatively, *Whi3*-mediated recruitment of many other mRNAs would localize their translation at the cytosolic face of the ER and/or contribute to an efficient translocation across the ER of those encoded proteins destined to the exocytic pathway.

source. Thus, *Whi3* could localize synthesis of *Aft1* for efficient regulation by ER-originated signals.

In addition to *CLN3*, we show that *Whi3* binds to mRNAs encoding other CDK regulators including B-type cyclins, kinase *Swe1*, and phosphatase *Mih1*. The regulation of CDK activity is associated with the ER compartment in different phases of the cell cycle. We have shown that the *Cdc28-Cln3* complex is retained at the ER until late  $G_1$ , where *Ssa1,2-Ydj1* chaperones release the complex and allow its nuclear accumulation to trigger cell cycle entry (20). In mammals, cyclin A is transiently maintained in the cytoplasm by retention at the ER cytoplasmic surface, and this retention is essential for cells to enter S phase adequately (47). Also, cyclin B2 appears to associate primarily with the Golgi apparatus, whereas cyclin B1 co-localizes with microtubules (48), where they may play important roles for ER and Golgi fragmentation during mitosis. The inhibition of the *Clb-Cdk1* activity by *Wee1* and *Myt1* kinases is essential for the reassembly of ER and Golgi during telophase and exit from mitosis (49). Thus, *Whi3* may play a role in localizing translation of the different CDK regulators on the ER to optimize functional interactions among them or with their targets.

It has been demonstrated that mRNA-binding proteins recognize specific *cis*-acting determinants within their targets, characterizing these common sequences a discrete subpopulation of messenger RNAs coordinately regulated (4, 50). The analysis of *Whi3* targets also revealed the presence of a *cis*-acting determinant for *Whi3* binding. First, clusters with four GCAU tetranucleotides were significantly enriched among the *Whi3* targets. Second, mutation of the



14 GCAU sites in the mRNA of *CLN3* caused a clear reduction in its interaction with Whi3. Nonetheless, removal of the GCAU sequences did not totally abolish the ability of Whi3 to bind the *CLN3* mRNA. This is not surprising as protein-RNA interactions frequently depend on different structural and/or sequence *cis*-determinants (50). Considering that a GCAU tetranucleotide can be bound by a single RRM domain, the enrichment in GCAU clusters suggests that Whi3 would form multimeric complexes on target mRNAs. Whi3 binds both its own and the *WHI4* mRNA (supplemental Table S1), which could contribute to produce local accumulations of these RNA-binding proteins and form multimeric complexes.

Fig. 7 depicts a speculative model representing the cellular roles of Whi3. The cytoplasmic surface of the ER is an essential compartment for protein sorting. Although recruitment of mRNAs to the ER should be a key first step, little is known about the determinants that anchor ribonucleoparticles to the ER surface. Indeed, Whi3 may itself be a determinant for ribonucleoparticle recruitment to the ER surface. In addition, Whi3 could be an adaptor for other regulators of its target-mRNA encoded proteins. For instance, we have found that Whi3 is associated to Ssa1,2 chaperones (19), which in turn are involved in protein translocation across the ER membrane (8, 11) and in ER retention/release of proteins (20, 45). Additional work will be required to uncover the precise molecular mechanisms by which Whi3 exerts local regulatory functions on such a plethora of target mRNAs.

*Acknowledgments*—We gratefully acknowledge Dhruba J. Sengupta, Stan Fields, and Marvin Wickens for communicating unpublished results. We thank Emili Vergès, Sònia Rius, and Isis Navarro for technical assistance. We thank Humberto Torres, Maria Molina, Felip Vilella, M<sup>a</sup> Angeles de la Torre, and Núria Pujol-Carrión for yeast strains and plasmids. Thanks also go to the members of CYC laboratory for helpful discussions.

**REFERENCES**

1. Moore, M. J. (2005) *Science* **309**, 1514–1518
2. Takizawa, P. A., DeRisi, J. L., Wilhelm, J. E., and Vale, R. D. (2000) *Science* **290**, 341–344
3. Tenenbaum, S. A., Carson, C. C., Lager, P. J., and Keene, J. D. (2000) *Proc. Natl. Acad. Sci. U. S. A.* **97**, 14085–14090
4. Keene, J. D. (2007) *Nat. Rev. Genet.* **8**, 533–543
5. Keene, J. D., and Tenenbaum, S. A. (2002) *Mol. Cell* **9**, 1161–1167
6. Jansen, R. P. (2001) *Nat. Rev. Mol. Cell Biol.* **2**, 247–256
7. St Johnston, D. (2005) *Nat. Rev. Mol. Cell Biol.* **6**, 363–375
8. Nicchitta, C. V., Lerner, R. S., Stephens, S. B., Dodd, R. D., and Pyhtila, B. (2005) *Biochem. Cell Biol.* **83**, 687–695
9. Diehn, M., Eisen, M. B., Botstein, D., and Brown, P. O. (2000) *Nat. Genet.* **25**, 58–62
10. Mutka, S. C., and Walter, P. (2001) *Mol. Biol. Cell* **12**, 577–588
11. Gerst, J. E. (2008) *Trends Cell Biol.* **18**, 68–76
12. Aronov, S., Gelin-Licht, R., Zipor, G., Haim, L., Safran, E., and Gerst, J. E. (2007) *Mol. Cell Biol.* **27**, 3441–3455
13. Schmid, M., Jaedicke, A., Du, T. G., and Jansen, R. P. (2006) *Curr. Biol.* **16**, 1538–1543
14. Shepard, K. A., Gerber, A. P., Jambhekar, A., Takizawa, P. A., Brown, P. O., Herschlag, D., DeRisi, J. L., and Vale, R. D. (2003) *Proc. Natl. Acad. Sci. U. S. A.* **100**, 11429–11434
15. Nash, R. S., Volpe, T., and Futcher, B. (2001) *Genetics* **157**, 1469–1480

16. Gari, E., Volpe, T., Wang, H., Gallego, C., Futcher, B., and Aldea, M. (2001) *Genes Dev.* **15**, 2803–2808
17. de Bruin, R. A., McDonald, W. H., Kalashnikova, T. I., Yates, J., III, and Wittenberg, C. (2004) *Cell* **117**, 887–898
18. Costanzo, M., Nishikawa, J. L., Tang, X., Millman, J. S., Schub, O., Breitkreuz, K., Dewar, D., Rupes, I., Andrews, B., and Tyers, M. (2004) *Cell* **117**, 899–913
19. Wang, H., Gari, E., Vergés, E., Gallego, C., and Aldea, M. (2004) *EMBO J.* **23**, 180–190
20. Verges, E., Colomina, N., Gari, E., Gallego, C., and Aldea, M. (2007) *Mol. Cell* **26**, 649–662
21. Sopko, R., Huang, D., Preston, N., Chua, G., Papp, B., Kafadar, K., Snyder, M., Oliver, S. G., Cyert, M., Hughes, T. R., Boone, C., and Andrews, B. (2006) *Mol. Cell* **21**, 319–330
22. Mosch, H. U., and Fink, G. R. (1997) *Genetics* **145**, 671–684
23. Gallego, C., Gari, E., Colomina, N., Herrero, E., and Aldea, M. (1997) *EMBO J.* **16**, 7196–7206
24. Gietz, D., St. Jean, A., Woods, R. A., and Schiestl, R. H. (1992) *Nucleic Acids Res.* **20**, 1425
25. Guthrie, C., and Fink, G. R. (eds) (1991) *Methods in enzymology*, Vol. 194, Academic Press, San Diego, CA
26. Wach, A., Brachat, A., Pohlmann, R., and Philippsen, P. (1994) *Yeast* **10**, 1793–1808
27. Ausubel, F. M., Brent, R., Kingston, R. E., Moore, D. D., Seidman, J. G., Smith, J. A., and Struhl, K. (eds) (1987) *Current Protocols in Molecular Biology*, John Wiley and Sons, Inc., Hoboken, NJ
28. Rigaut, G., Shevchenko, A., Rutz, B., Wilm, M., Mann, M., and Séraphin, B. (1999) *Nat. Biotech.* **10**, 1030–1032
29. DeRisi, J. In Bowtell, D., and Sambrook, J. (2002) *DNA Microarrays: A Molecular Cloning Manual*, pp. 187–193, Cold Spring Harbor Laboratory, Cold Spring Harbor, NY
30. Spellman, P. T., Sherlock, G., Zhang, M. Q., Iyer, V. R., Anders, K., Eisen, M. B., Brown, P. O., Botstein, D., and Futcher, B. (1998) *Mol. Biol. Cell* **9**, 3273–3297
31. Montaner, D., Tárrega, J., Huerta-Cepas, J., Burguet, J., Vaquerizas, J. M., Conde, L., Minguez, P., Vera, J., Mukherjee, S., Valls, J., Pujana, M. A., Alloza, E., Herrero, J., Al-Shahrour, F., and Dopazo, J. (2006) *Nucleic Acids Res.* **34**, W486–491
32. de la Torre-Ruiz, M. A., Torres, J., Ariño, J., and Herrero, E. (2002) *J. Biol. Chem.* **277**, 33468–33476
33. Gerber, A. P., Herschlag, D., and Brown, P. O. (2004) *PLoS Biol.* **2**, 342–354
34. Mewes, H. W., Dietmann, S., Frishman, D., Gregory, R., Mannhaupt, G., Mayer, K. F., Münsterkötter, M., Ruepp, A., Spannagl, M., Stümpflen, V., and Rattei, T. *Nucleic Acids Res.* (2008) **36**, D196–D201
35. Issel-Tarver, L., Christie, K. R., Dolinski, K., Andrada, R., Balakrishnan, R., Ball, C. A., Binkley, G., Dong, S., Dwight, S. S., Fisk, D. G., Harris, M., Schroeder, M., Sethuraman, A., Tse, K., Weng, S., Botstein, D., and Cherry, J. M. (2002) *Methods Enzymol.* **350**, 329–346
36. Kumar, A., Agarwal, S., Heyman, J. A., Matson, S., Heidtman, M., Piccirillo, S., Umansky, L., Drawid, A., Jansen, R., Liu, Y., Cheung, K. H., Miller, P., Gerstein, M., Roeder, G. S., and Snyder, M. (2002) *Genes Dev.* **16**, 707–719
37. Lesage, G., and Bussey, H. (2006) *Microbiol. Mol. Biol. Rev.* **70**, 317–343
38. Jin, Q. W., and McCollum, D. (2003) *Eukaryot. Cell* **2**, 510–520
39. Karagiannis, J., Oulton, R., and Young, P. G. (2002) *Genetics* **162**, 45–58
40. Maris, C., Dominguez, C., and Allain, F. H. (2005) *FEBS J.* **272**, 2118–2131
41. SenGupta, D. J., Zhang, B., Kraemer, B., Pochart, P., Fields, S., and Wickens, M. (1996) *Proc. Natl. Acad. Sci. U. S. A.* **93**, 8496–8501
42. Sengupta, D. J., Wickens, M., and Fields, S. (1999) *RNA* **5**, 596–601
43. Zurita-Martinez, S. A., Puria, R., Pan, X., Boeke, J. D., and Cardenas, M. E. (2007) *Genetics* **176**, 2139–2150
44. Prinz, S., Aldridge, C., Ramsey, S. A., Taylor, R. J., and Galitski, T. (2007) *PLoS ONE* **2**, e249
45. Hoppe, T., Matuschewski, K., Rape, M., Schlenker, S., Ulrich, H. D., and Jentsch, S. (2000) *Cell* **102**, 577–586
46. Philpott, C. C., and Protchenko, O. (2008) *Eukaryot. Cell* **7**, 20–27

47. Tsang, W. Y., Wang, L., Chen, Z., Sánchez, I., and Dynlacht, B. D. (2007) *J. Cell Biol.* **178**, 621–633
48. Jackman, M., Firth, M., and Pines, J. (1995) *EMBO J.* **14**, 1646–1654
49. Nakajima, H., Yonemura, S., Murata, M., Nakamura, N., Pivnicka-Worms, H., and Nishida, E. (2008) *J. Cell Biol.* **181**, 89–103
50. Jambhekar, A., and DeRisi, J. L. (2007) *RNA* **13**, 625–642
51. Eisen, M. B., Spellman, P. T., Brown, P. O., and Botstein, D. (1998) *Proc. Natl. Acad. Sci. U. S. A.* **95**, 14863–14868
52. Robinson, M. D., Grigull, J., Mohammad, N., and Hughes, T. R. (2002) *BMC Bioinformatics* **3**, 35
53. Letunic, I., Copley, R. R., Pils, B., Pinkert, S., Schultz, J., and Bork, P. *Nucleic Acids Res.* (2006) **34**, D257–D260